

Mesenchymal Stem Cell Time to Confluence on 3D Printed, Porous, Poly(propylene fumarate)
Scaffolds for Bone Tissue Engineering

Undergraduate Honors Research Thesis

Presented in Partial Fulfillment of the Requirements for the Bachelor of Science with Honors
Research Distinction in the College of Engineering of The Ohio State University

By

Ryan Andrew McIlvaine

The Ohio State University

April 2022

Honors Thesis Committee

Dr. David Dean, Advisor

Dr. Derek Hansford

| | |
|--------------------------------|----|
| Table of Contents | |
| Abstract | 3 |
| Acknowledgements | 4 |
| List of Figures | 5 |
| Introduction | 6 |
| Methods | 8 |
| Experimental Design | 8 |
| Scaffold 3D Printing..... | 8 |
| Cell Culture & Suspension..... | 9 |
| Scaffold Seeding | 10 |
| SEM Preparation & Imaging..... | 10 |
| Results | 11 |
| Dropwise Method..... | 11 |
| Top-down Method..... | 14 |
| Sectioned Scaffolds | 15 |
| Discussion | 16 |
| Conclusion | 17 |
| References | 18 |

Abstract

Autologous bone grafting is the standard-of-care procedure for treating bone defects above critical-size. Current research shows that a tissue engineering solution may offer a better pathway for healing bone defects. This project focuses on the union of the three pillars of tissue engineering, namely a material scaffold, cell line, and growth factors, to work towards a proper solution. Specifically, we investigate the time to confluence of bone marrow-derived human mesenchymal stem cells (BM-hMSCs) seeded onto 3D printed poly(propylene fumarate) (PPF) scaffolds with a gyroid pore geometry. BM-hMSCs were seeded using a dropwise method onto scaffolds of two different geometries (coarse and fine) and cultured over a period of 28 days; two scaffolds were set aside and seeded using a top-down method. SEM images were collected on Day 1, 7, and 28. These images demonstrate a gradual proliferation and migration of cells over the scaffold, eventually covering all exterior struts as well as bridging the exterior pores of both the fine and coarse geometry scaffolds. The Day 28 scaffolds were sectioned across the narrow width of the scaffold and the interior was also imaged. These images displayed cell growth throughout the interior of the scaffold throughout the pore space, which can be seen for both geometries. Finally, when examining the top-down scaffolds, we note a lack of full confluence on the coarse geometry scaffold. This is an indication that the lack of even cell distribution during seeding prevents cell migration across the entire scaffold in the same time period as those seeded with the dropwise method. This data ultimately indicates the success of the dropwise seeding method and the efficacy of the use of PPF as BM-hMSC scaffolds. With this work, we look to reproduce these results with an increased time resolution and explore the ability to differentiate these cells when seeded on these scaffolds.

Acknowledgements

I would like to thank my research advisor, Dr. David Dean, for supporting me throughout this extremely valuable and rewarding research process. I'm extremely grateful for his support throughout the many challenges faced during this project and his help in formulating my post-graduate plans. I'd also like to thank Ryan Hooper for being an immense resource during my work in our lab; his help was invaluable. I'm grateful for Dr. Daniel Veghte, who was a great asset in training me to perform electron microscopy at the Center for Electron Microscopy and Analysis (CEMAS). I'm very grateful for the generous funding I received from a summer 2022 URAP scholarship, a summer 2022 STEP scholarship, and a College of Engineering Undergraduate Research Scholarship. Partial support was provided by the DoD AFIRM II effort under award No. W81XWH-14-2-0004 and Osteo Science Foundation award No. 110850. I'd like to thank the department of Biomedical Engineering for the fantastic instruction they've given me, especially Dr. Derek Hansford, who has taught several of my courses and generously agreed to join my thesis committee. Lastly, to my family and my friends, especially Emma, Tommy, Sydney, Giacomo, and Adam, thank you for your unwavering support.

List of Figures

Figure 1. Day 1 Scaffolds. 12
Figure 2. Day 7 Scaffolds 13
Figure 3. Day 28 Coarse Scaffolds 13
Figure 4. Day 28 Fine Scaffolds 14
Figure 5. Day 28 Top-Down Scaffolds..... 15
Figure 6. Day 28 Sectioned Scaffolds..... 16

Introduction

Despite decades of research, autologous bone graft tissue remains the standard-of-care source of bone for critical-size bone defects (i.e., bone defects that are too large to heal unaided) (Schmitz & Hollinger, 1986). Bone tissue engineering aims to use regenerative technology to address current limitations in bone healing by creating “artificial bone” for use in critical-size and larger defects. These methods typically involve drugs and artificial bone cement or bone fillers alongside tissue transplantation, which can introduce various limitations such as a higher cost due to the surgery required, loss of bone at the donor site, increased risk of patient infection or death, and a limited supply of available tissue. (Amini, Laurencin, & Nukavarapu, 2012). Therefore, tissue engineering offers another route to solving these problems, namely from 3 main categories: cells and cell sources, cell scaffolds, and growth factors (Mistry & Mikos, 2005). This study focuses on the efficacy of the union of these three categories into a single engineered solution for critical-size bone defects.

A number of biomaterials have been investigated for use in bone tissue engineering and can be categorized into a few distinct classes: metals, ceramics, and polymers. Polymers have been the most extensively studied for tissue engineering scaffolds. While metals have been extensively used for bone healing solutions, they are a poor choice for cell scaffolds, and only a select few alloys are safely biodegradable (Bose, Roy, & Bandyopadhyay, 2012). Ceramics are a popular choice in bone tissue engineering solutions and can also successfully be 3D printed. However, they can be incredibly brittle and often are non-biocompatible due to leeching of the material over time (Ginebra, Espanol, Maazouz, Bergez, & Pastorino, 2018). Specifically, some of the most common polymers are poly(glycolic acid) (PGA), poly(lactic acid) (PLA), poly(caprolactone) (PCL), collagen, and poly(propylene fumarate) (PPF), to name a few. PPF is a resorbable photo-cross-

linkable polymer that can be successfully fabricated into geometries using 3D printing (digital light processing, DLP) (Dean, et al., 2012). The polymer can also be modified to allow for increased cell adhesion and biocompatibility (Dean, et al., 2003) (Fisher, Dean, & Mikos, 2002) (Wang, et al., 2015). In this study, we investigate the use of PPF scaffolds of two different Schoen's gyroid (i.e., gyroid) pore geometries. This gyroid geometry is designed so that there is a relatively uniform distribution of material (i.e., no large bulk areas) that provides uniform access to fluid flow throughout the scaffold (Günther, Wagner, Pilz, Gebert, & Zimmermann, 2021). This porosity is important, as there needs to be enough room for cell nutrient and waste flow to occur inside this scaffold, as well as uniform degradation of the scaffold by hydrolysis.

While a variety of cell types have been investigated, bone marrow-derived human mesenchymal stem cells (BM-hMSCs) have become a favored choice for bone tissue engineering (Abdi, Fiorina, Adra, Atkinson, & Ssayegh, 2008) (Ma, et al., 2013). These cells are multipotent adult stem cells that can be differentiated into different mesoderm-type cells such as adipocytes and osteoblasts (Abdallah & Kassem, 2008). This differentiation can be controlled through a detailed sequence of cellular factors included in the cell media. These cells are relatively easy to work with *in vitro* compared to other precursor cell options and offer a good choice for tissue engineering applications.

In a prior study, select concentrations of epidermal growth factor (EGF), fibroblast growth factor (FGF), and platelet-derived growth factor (PDGF) have been established to enhance the proliferation and growth of the BM-MSCs (Eom, et al., 2014) (Mishra, et al., 2016). We utilize a proliferation media composed of these growth factors in this study, alongside printed PPF scaffolds seeded with BM-hMSCs.

In order to further study the use of this tissue engineering solution and its potential as a clinical tool, a deeper understanding of the seeding and proliferation of cells on these scaffolds is required. We know proliferation will only occur after cells have attached to the scaffold; newly proliferated cells are likely to attach near to where they derive. However, we have yet to determine the time to confluence of the cells in regard to the different geometries. Thus, in this study, we investigate the efficacy and time to confluence of BM-hMSCs on PPF scaffolds.

Methods

Experimental Design

Twelve ($N=12$) PPF scaffolds 6 mm in diameter and 10 mm in length were printed via the method outlined below. These scaffolds were seeded with BM-hMSCs before being incubated over a 28-day period. On day 1, 7, and 28, four scaffolds were removed and SEM images were collected to observe the cell growth over time. Two of the four scaffolds intended for day 28 were set aside to utilize a top-down seeding method, as opposed to the dropwise method used for the other scaffold; these methods can be found below.

Scaffold 3D Printing

PPF resin was obtained from the laboratory of Dr. Matthew Becker, Duke University (Durham, NC). The resin is stirred using a stir motor for 12 hours (overnight) at 30°C. The EnvisionTEC Perfactory® P3 3D printer (Dearborn, MI) is calibrated and the print file of the porous cylindrical scaffolds with gyroid geometry is uploaded to print the structures. Six ($N=6$) scaffolds of a coarse geometry (400 μm struts and 1400 μm pores) and 6 of a fine geometry (200

µm struts and 700 µm pores) were printed. The basement of the printer is cleaned, and the leftover resin collected, followed by a final wash of ethanol.

To wash the scaffolds, they are rinsed with 70% acetone (VWR, PA) for 5 seconds, followed by ethanol for 5 seconds and then distilled water for 5 seconds followed by drying with compressed air. This process is repeated twice for a total of 3 times. The scaffolds are then cured for 8 hours in a UV oven (3D Systems, SC).

Cell Culture & Suspension

BM-hMSCs (MSC-003; RoosterBio, Inc., Frederick, MD) were revived at passage number 3 and cultured in a T-125 cell culture flask for 6 days in an incubator set to 37°C in >95% humidity and 5% CO₂. Revival media was created using basal media (KT-001; RoosterBio, Inc. MD) alongside penicillin streptomycin (Pen Strep) (Thermo Fisher Scientific Inc., MA). The proliferation media used for seeding was basal media supplemented with FGF, PDGF, and EGF (PeproTech, NJ). Media was changed every 2 days before being passaged at approximately 80% confluence on Day 6.

To passage and prepare the cell suspension, the cell culture was washed twice with phosphate-buffered saline (PBS) (Thermo Fisher Scientific Inc., MA) and then exposed to TrypLE Select (1X) (Thermo Fisher Scientific Inc., MA) and incubated for 5 minutes. Once the cells no longer adhered to the bottom of the culture flask, revival media was added to dilute the TrypLE. The contents of the flask were transferred to a 50-mL conical tube and centrifuged for 5 minutes at 1200 RPM. The liquid remainder was aspirated out, and the cell pellet was resuspended in proliferation media to create a concentration of 1 million cells per 90 µL of solution.

Scaffold Seeding

To prepare and sterilize scaffolds before seeding, a solution of 21% acetone, 49% ethanol, and 30% distilled water was created. The scaffolds were soaked in PBS for 5 minutes before being removed and placed in a bath of the acetone solution for 25 minutes. The scaffolds were then removed and placed in a new PBS soak every 5 minutes for a total of 15 minutes, or 3 consecutive soaks. Then, the scaffolds soaked in a new bath of acetone solution for 25 minutes and before being washed with an additional 3 soaks for PBS. Finally, the scaffolds were autoclaved in a glass jar before being soaked in basal media for 48 hours.

Ten ($n=10$) scaffolds were seeded using a manual, dropwise seeding method, and two ($n=2$) additional scaffolds, one of each geometry, were seeded using a top-down method. Both methods involve seeding 90 μL of a 1 million cell suspension of each fine scaffold. This suspension is diluted to 500,000 cells per 90 μL to then be used for the coarse scaffolds. To seed via the dropwise method, a micropipette is used to seed individual drops along the surfaces of the scaffold; approximately one drop on each end, and five drops around the circumferential surface. To seed via the drop-down method, the entire 90 μL is deposited on one end of the scaffold.

Each seeded scaffold was placed in a 12-well ultra-low attachment well plate well and incubated at 37°C and 5% CO_2 for 5 hours to allow the cells to attach. Each scaffold was then submerged in proliferation media and replaced back in the incubator.

SEM Preparation & Imaging

Scaffolds were prepared for SEM imaging via alcohol dehydration and glutaraldehyde fixation. A 1% glutaraldehyde solution is created with 0.1 M pH 7.4 PBS. Media in the well plates and scaffolds is aspirated out, and the scaffolds are washed twice with PBS. 1.2 mL of the glutaraldehyde solution is placed in each well to submerge the scaffolds for 30 minutes. The

glutaraldehyde was removed, and PBS was used to rinse the scaffolds. They are then submerged in a 50% ethanol solution for 5 minutes. This solution is removed and replaced with a fresh 50% ethanol solution for another 5 minutes. This process is repeated with a 70%, 80%, 95% and 100% ethanol solution, with one extra submersion of the 100% ethanol solution. Finally, the scaffolds are placed in a 100% HMDS (Sigma-Aldrich, MO) solution for 5 minutes. They are then removed and blotted dry, before being stored in a desiccator until sputter coating.

Samples are mounted on SEM stubs before being sputter coated with gold plasma (Pelco, CA) to enhance SEM imaging.

Scaffolds collected on Day 28 were sectioned horizontally via razor blade through the narrow dimension of the scaffold after imaging, and were re-sputter coated and imaged following the protocols explained above.

These samples were viewed and imaged using a Quattro ESEM scanning electron microscope (Thermo Fisher Scientific Inc., MA) with a voltage of 5.00 kV and a working distance from 10 to 20 mm.

Results

Dropwise Method

The SEM images collected on day 1 are shown in Figure 1, where only a small number of cells can be seen attached to the scaffold, with some spreading. At this resolution, the print-lines of both scaffold geometries can also be seen.

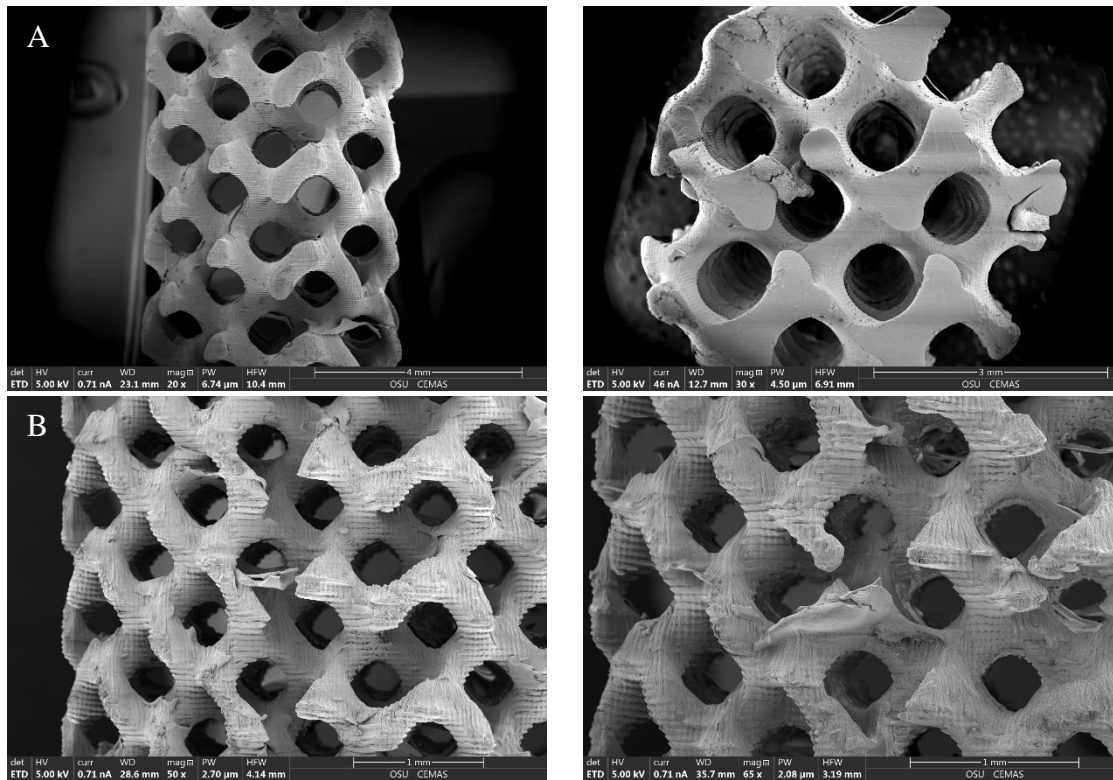


Figure 1. Day 1 Scaffolds. (A) Coarse geometry scaffolds 24 hours post-seeding. (B) Fine geometry scaffolds 24-hours post seeding.

The scaffolds imaged on day 7 and 28 can be seen in Figure 2, and Figures 3 and 4, respectively. There is a notable difference between day 1 and day 7, and day 7 and day 28. Day 7 scaffolds demonstrate a much more expansive cell coverage- cells begin to coat the struts of the scaffold, and pseudopodia can be seen as the cells attempt to anchor across surfaces and begin to bridge the pores of the structure. Finally, scaffolds imaged on day 28 show full or nearly full confluence (i.e., complete coverage of all surfaces) on both scaffold geometries. The cells have branched across all exposed pores on the exterior of the scaffold to form a cohesive layer.

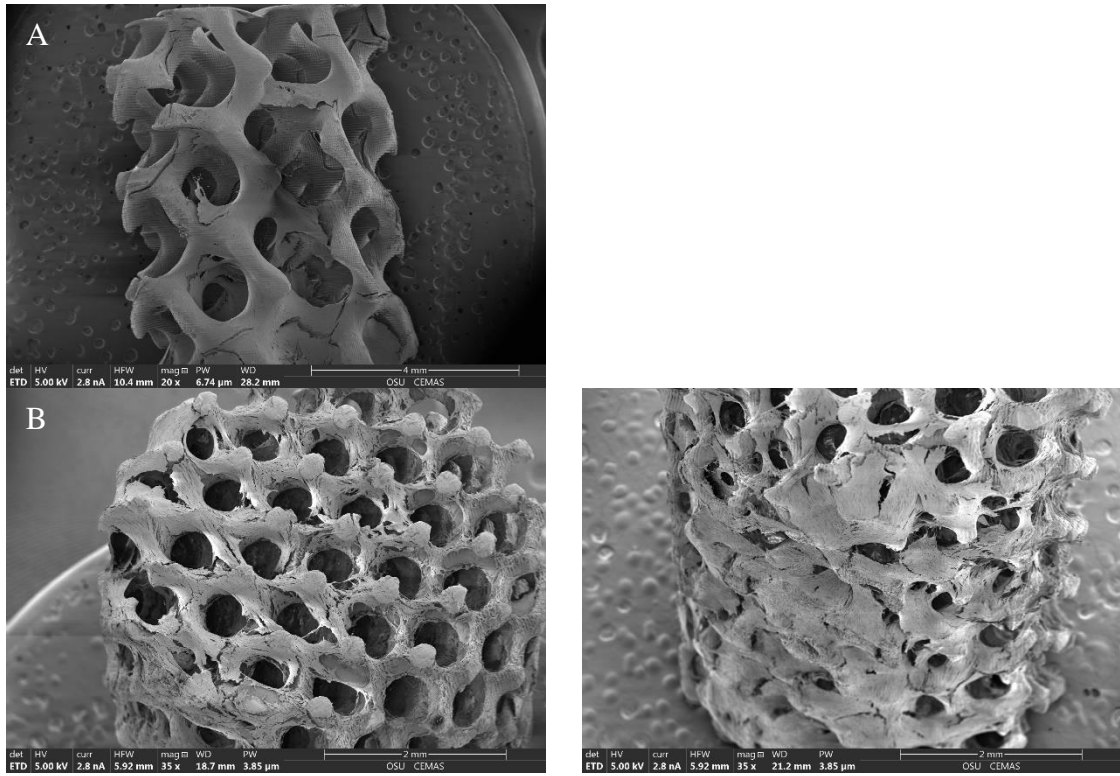


Figure 2. Day 7 Scaffolds. (A) Coarse geometry scaffolds 7 days post-seeding. (B) Fine geometry scaffolds 7 days post-seeding.

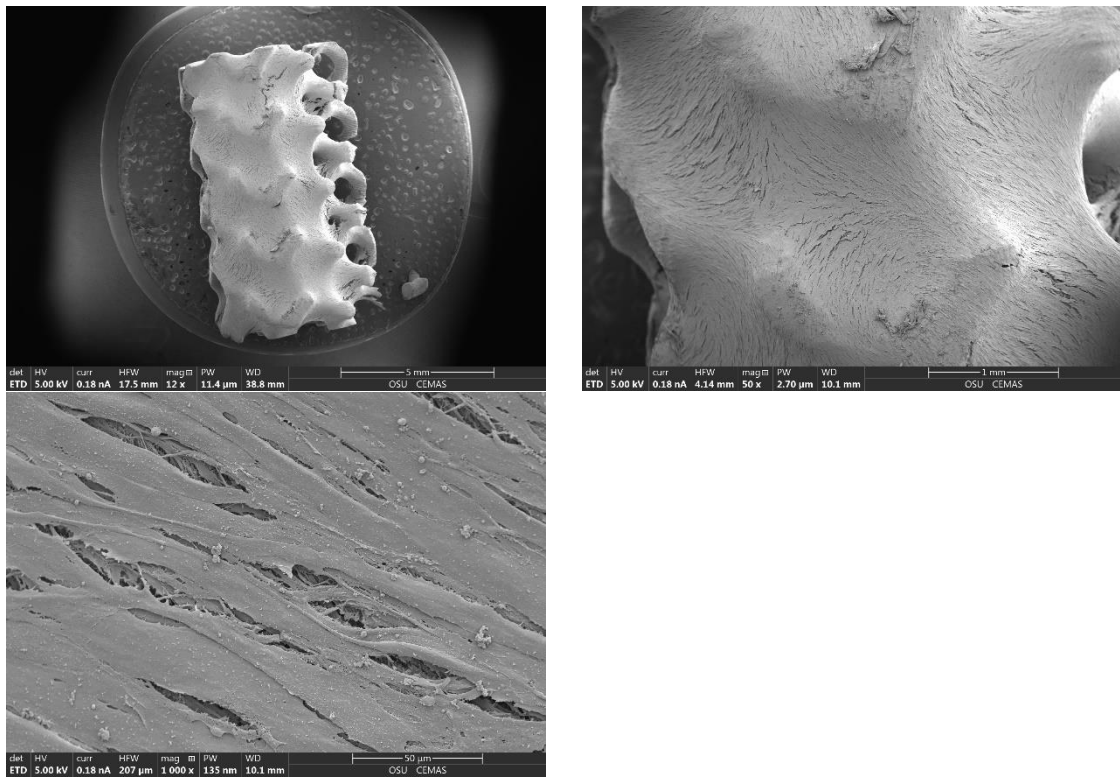


Figure 3. Day 28 Coarse Scaffolds. Coarse geometry scaffolds 28 days post-seeding.

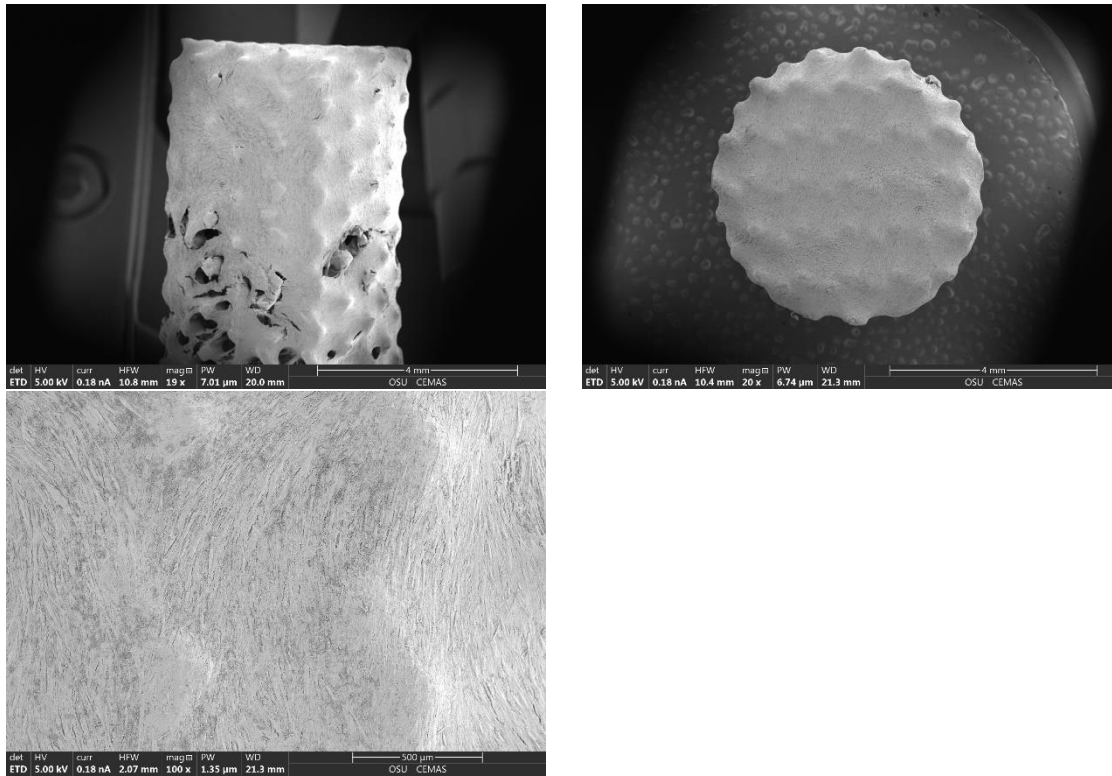


Figure 4. Day 28 Fine Scaffolds. Fine geometry scaffolds 28 days post-seeding.

Top-down Method

The other 2 scaffolds collected on day 28 were seeded using the top-down method. The fine scaffold demonstrated a similar confluence to the dropwise method. However, the coarse scaffold seeded in this manner only demonstrated partial confluence, particularly focused on one end of the scaffold, as seen in Figure 5.

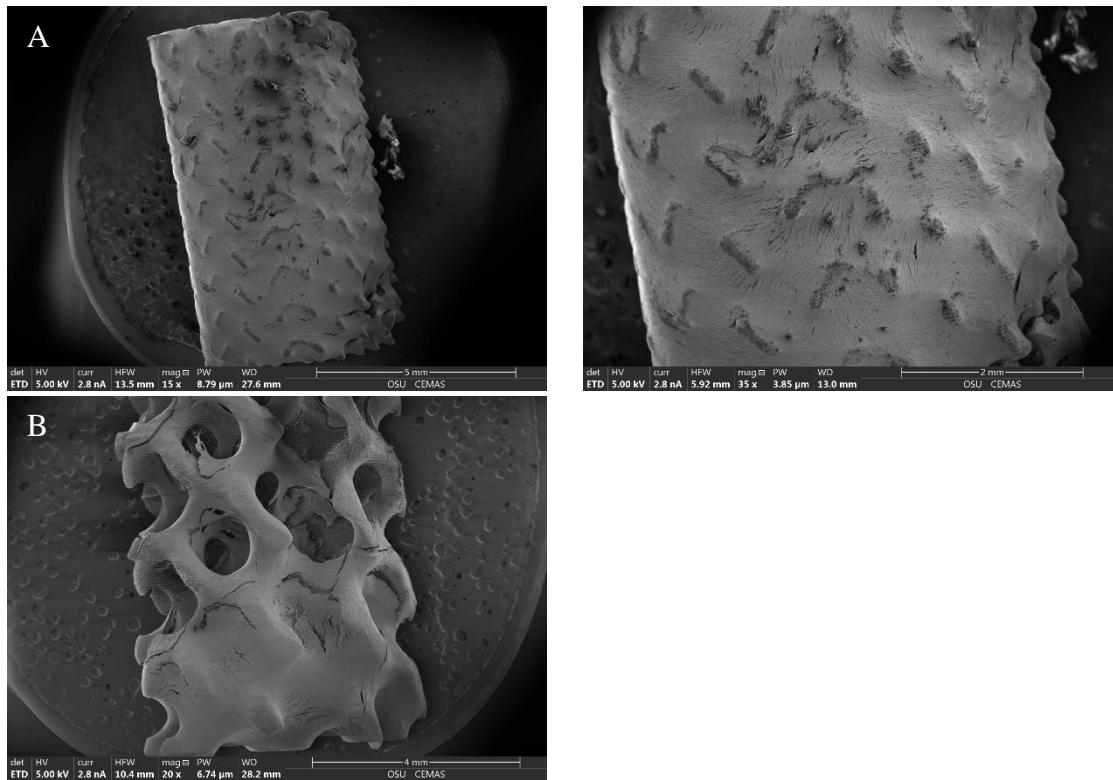


Figure 5. Day 28 Top-Down Scaffolds. (A) Fine geometry scaffold seeded via the top-down method. (B) Coarse geometry scaffold seeded via the top-down method.

Sectioned Scaffolds

To ensure that cell proliferation extended to inside of the scaffolds, SEM images of the sections of the day 28 dropwise scaffolds can be seen in Figure 6. Cells are shown to have migrated inside the scaffold and proliferated well, though not to the same capacity of the cells on the exterior of the scaffold.

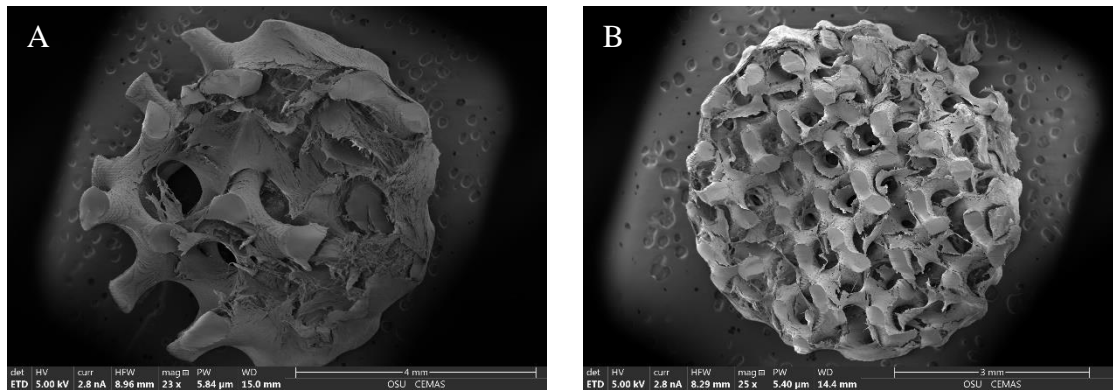


Figure 6. Day 28 Sectioned Scaffolds. (A) Coarse geometry scaffold sectioned on day 28. (B) Fine geometry scaffold sectioned on day 28.

Discussion

The SEM images collected show a distinct level of progress towards confluence over the 28-day period. Most notably, there is an apparent confluence of the scaffolds at day 28; the scaffold geometry is still visible under a dense layer of cells and ECM. It is also important to note the success of the manual seeding technique. Gaps (i.e., areas of the scaffold surface had no cells) were observed in cell coverage in the scaffolds seeded with the top-down method, but very few were seen in the dropwise method scaffolds. The gaps seen in the top-down method are most likely a result of the cell's lack of migratory ability to reach the end of the scaffold from the initial seeding location. However, the images of sections of the day 28 dropwise scaffolds indicated cell growth in the inner pores of the scaffolds of both geometries; this indicates that there is sufficient flow to the inside of the scaffold, allowing for cells that were originally attached to proliferate inside, as well as supporting cell migration in that direction, even as the cell layer on the exterior continued to grow.

Conclusion

The success of the manual seeding protocol in reaching confluence at the final time point (i.e., full coating of the scaffold surface) now leads us to investigate the differences, if any, in speed of obtaining confluence for the two scaffold architectures and the nature of the resulting ECM. Given the observations of this study, it may not be necessary to conduct a 28 day protocol, not only because of its length but because of the increased risk of contamination. Given that 21 days is at the long end of a cell-based therapy protocol, it would be useful to include more time points between days 2 and 14. In order for these scaffolds to be useful in a clinical setting, the seeded and coated cells must be functional after the attached cells differentiate to the bone lineage. Indeed, a question of how the coating of undifferentiated stem cells relates to the quality of the ECM secreted and mineralized under differentiation media. It is important to maintain a structure that can be remodeled and vascularized.

References

- Abdallah, B. M., & Kassem, M. (2008). Human mesenchymal stem cells: from basic biology to clinical applications. *Gene Therapy*, 109-116.
- Abdi, R., Fiorina, P., Adra, C. N., Atkinson, M., & Ssayegh, M. H. (2008). Immunomodulation by mesenchymal stem cells: a potential therapeutic strategy for type 1 diabetes. *Diabetes*, 1759-1767.
- Amini, R. A., Laurencin, C. T., & Nukavarapu, S. P. (2012). Bone Tissue Engineering: Recent Advances and Challenges. *Critical Reviews in Biomedical Engineering*, 363-408.
- Bose, S., Roy, M., & Bandyopadhyay, A. (2012). Recent advances in bone tissue engineering scaffolds Susmita. *Trends in Biotechnology*, 546-554.
- Dean, D., Topham, N. S., Meneghetti, S. C., Wolfe, M. S., Jepsen, K., He, S., . . . Mikos, A. G. (2003). Poly(propylene fumarate) and poly(DL-lactic-co-glycolic acid) as scaffold materials for solid and foam-coated composite tissue-engineered constructs for cranial reconstruction. *Tissue Engineering*, 495-504.
- Dean, D., Wallace, J., Siblani, A., Wang, M. O., Kim, K., Mikos, A. G., & Fisher, J. P. (2012). Continuous Digital Light Processing (cDLP): Highly Accurate Additive Manufacturing of Tissue Engineered Bone Scaffolds. *Virtual & Physical Prototyping*, 13-24.
- Eom, Y. W., Oh, J.-E., Lee, J. I., Baik, S. K., Rhee, K.-J., Shin, H. C., . . . Shim, K. Y. (2014). The role of growth factors in maintenance of stemness in bone marrow-derived mesenchymal stem cells. *Biochemical and Biophysical Research Communications*, 16-22.
- Fisher, J. P., Dean, D., & Mikos, A. G. (2002). Photocrosslinking characteristics and mechanical properties of diethyl fumarate/poly(propylene fumarate) biomaterials. *Biomaterials*, 4333-4343.
- Ginebra, M.-P., Espanol, M., Maazouz, Y., Bergez, V., & Pastorino, D. (2018). Bioceramics and bone healing. *EFORT Open Reviews*, 173-183.
- Günther, F., Wagner, M., Pilz, S., Gebert, A., & Zimmermann, M. (2021). Design procedure for triply periodic minimal surface based biomimetic scaffolds. *Journal of the Mechanical Behavior of Biomedical Materials*.
- Ma, S., Xie, N., Li, W., Yuan, B., Shi, Y., & Wang, Y. (2013). Immunobiology of mesenchymal stem cells. *Cell Death & Differentiation*, 216-225.
- Mishra, R., Sefcik, R. S., Bisop, T. J., Montelone, S. M., Crouser, N., Welter, J. F., . . . Dean, D. (2016). Growth Factor Dose Tuning for Bone Progenitor Cell Proliferation and Differentiation on Resorbable Poly(propylene fumarate) Scaffolds. *Tissue Engineering - Part C: Methods*, 904-913.
- Mistry, A. S., & Mikos, A. G. (2005). Tissue engineering strategies for bone regeneration. *Advances in Biochemical Engineering/Biotechnology*, 1-22.

- Schmitz, J. P., & Hollinger, J. O. (1986). The critical size defect as an experimental model for craniomandibulofacial nonunions. *Clinical Orthopedics and Related Research*, 299-308.
- Wang, M. O., Vorwald, C. E., Dreher, M. L., Mott, E. J., Cheng, M.-H., Cinar, A., . . . Fisher, J. P. (2015). Evaluating 3D-printed biomaterials as scaffolds for vascularized bone tissue engineering. *Advanced Materials*, 138-144.